Article

A Novel Anti-CD44 variant 9 Monoclonal Antibody C44Mab-1 was developed for immunohistochemical analyses against colorectal cancers

Mayuki Tawara [1,#], Hiroyuki Suzuki [1*,#], Tomohiro Tanaka [1], Mika K. Kaneko [1,2], and Yukinari Kato [1,2*]

[1] Department of Molecular Pharmacology, Tohoku University Graduate School of Medicine, 2-1 Seiryo-machi, Aoba-ku, Sendai 980-8575, Miyagi, Japan; tawara.mayuki.p8@dc.tohoku.ac.jp (M.T.); tomohiro.tanaka.b5@tohoku.ac.jp (T.T.)

[2] Department of Antibody Drug Development, Tohoku University Graduate School of Medicine, 2-1 Seiryo-machi, Aoba-ku, Sendai 980-8575, Japan; k.mika@med.tohoku.ac.jp (M.K.K.)

* Correspondence: hiroyuki.suzuki.b4@tohoku.ac.jp (H.S.); yukinari.kato.e6@tohoku.ac.jp (Y.K.); Tel.: +81-22-717-8207 (H.S. and Y.K.)

[#]contributed equally to this work

Abstract: Cluster of differentiation 44 (CD44) is a type I transmembrane glycoprotein, and has been shown as a cell surface marker of cancer stem-like cells in various cancers. Especially, the splicing variants of CD44 (CD44v) are overexpressed in cancers, and play critical roles in cancer stemness, invasiveness, and resistance to chemotherapy and radiotherapy. Therefore, the understanding of the function of each CD44v is indispensable for the CD44-targeting therapy. CD44v9 contains the variant 9-encoded region, and its expression predicts poor prognosis in patients with various cancers. CD44v9 plays critical roles in the malignant progression of tumors. Therefore, CD44v9 is a promising target for cancer diagnosis and therapy. Here, we developed sensitive and specific monoclonal antibodies (mAbs) against CD44 by immunizing mice with CD44v3–10-overexpressed Chinese hamster ovary CHO-K1 (CHO/CD44v3–10) cells. We first determined their critical epitopes using enzyme-linked immunosorbent assay, and characterize their applications to flow cytometry, western blotting, and immunohistochemistry. One of the established clones, C44Mab-1 (IgG_1, kappa) reacted with a peptide of the variant 9-encoded region, indicating that C44Mab-1 recognizes CD44v9. C44Mab-1 reacted with CHO/CD44v3–10 cells or colorectal cancer cell lines (COLO201 and COLO205) by flow cytometry. The apparent dissociation constant (K_D) of C44Mab-1 for CHO/CD44v3–10, COLO201, and COLO205 was 2.5×10^{-8} M, 3.3×10^{-8} M, and 6.5×10^{-8} M, respectively. Furthermore, C44Mab-1 was able to detect the CD44v3–10 in western blotting, and endogenous CD44v9 in immunohistochemistry using colorectal cancer tissues. These results indicated that C44Mab-1 is useful for detecting CD44v9 not only in flow cytometry or western blotting but also in immunohistochemistry against colorectal cancers.

Keywords: CD44; CD44v9; monoclonal antibody; colorectal cancer

1. Introduction

Cluster of Differentiation 44 (CD44) is a type I transmembrane glycoprotein, and its variety of isoforms are expressed in various type of cells. [1]. The alternative splicing of CD44 mRNA mediates the variety of isoforms [2]. The CD44 standard (CD44s) isoform, the smallest isoform of CD44, is expressed in most vertebrate cells. CD44s mRNA is assembled by the first five (1 to 5) and the last five (16 to 20) constant region exons [3]. The CD44 variant (CD44v) isoforms are assembled by the alternative splicing of middle variant exons (v1–v10) in various combinations with the standard exons of CD44s [4]. Both CD44s and CD44v (pan-CD44) bind to hyaluronic acid (HA), which plays critical roles in cellular adhesion, migration, homing, and proliferation [5].

 doi:10.20944/preprints202303.0399.v1

The CD44 protein is further modified by variety of glycosylation, including *N*-glycans, *O*-glycans, and glycosaminoglycans（heparan sulphate, etc.）[6]. Due to the post-translational modifications, the molecular weight of CD44s is enlarged to 80–100 kDa, and some CD44v isoforms surpass 200 kDa due to a high level of glycosylation [7].

Several isoforms of the CD44 are associated with malignant progression in various tumors [8], including head and neck squamous cell carcinomas (SCCs) [9], pancreatic cancers [10,11], breast cancers [12], gliomas [13,14], prostate cancers [15], and colorectal cancers (CRC) [16]. CD44 is also known as a cell surface marker of cancer stem-like cells (CSCs) in various carcinomas [17]. Specific monoclonal antibodies (mAbs) to CD44s or CD44v are utilized for sorting $CD44^{high}$ CSCs [17]. The $CD44^{high}$ population exhibited the increased stemness property, drug resistance, and tumor formation *in vivo* [17]. Therefore, development of anti-CD44 mAbs, which recognize each variant, is important for the further characterization of CSCs in various cancers.

The functions of CD44v have been reported in the promotion of tumor invasion, metastasis, CSC properties [18], and resistance to chemotherapy and radiotherapy [8,19]. The v3-encoded region is modified by heparan sulfate, which promotes the binding to heparin-binding growth factors including fibroblast growth factors and heparin-binding epidermal growth factor-like growth factor. Therefore, the v3-encoded region functions as a co-receptor of receptor tyrosine kinases and potentiate their signal transduction [20]. Furthermore, the v6-encoded region is essential for the activation of c-MET through ternary complex formation with the ligand hepatocyte growth factor [21]. The v8–10-encoded region could bind to and stabilize a cystine–glutamate transporter (xCT), which promotes the defense to reactive oxygen species (ROS) via cystine uptake-mediated glutathione synthesis [22]. The regulation of redox status depends on the expression of CD44v8–10 that is associated with the xCT function and links to the poor prognosis of patients [23]. Therefore, the establishment and characterization of mAbs, which recognize each CD44v, are essential for understanding each variant function and development of CD44-targeting cancer therapy. However, the function and distribution of the variant 9-encoded region in tumors have not been fully understood.

We previously developed an anti-pan-CD44 mAb, C_{44}Mab-5 (IgG_1, kappa) [24] using the Cell-Based Immunization and Screening (CBIS) method. Furthermore, another anti-pan-CD44 mAb, C_{44}Mab-46 (IgG_1, kappa) [25] was established by immunizing mice with CD44v3–10 ectodomain. We showed that both C_{44}Mab-5 and C_{44}Mab-46 could be applied to flow cytometry and immunohistochemistry in oral [24] and esophageal SCCs [25]. We also determined the epitopes of C_{44}Mab-5 and C_{44}Mab-46 within the standard exons (1 to 5)-encoding regions [26-28]. Furthermore, we produced a defucosylated version (5-mG_{2a}-f) using FUT8-deficient ExpiCHO-S cells (BINDS-09) and investigated the antitumor effects of 5-mG_{2a}-f in mouse xenograft models of oral SCC [29]. Recently, we have been established various CD44v mAbs, including C_{44}Mab-108 (v4) [30] and C_{44}Mab-9 (v6) [31].

In this study, we established a novel anti-CD44v9 mAb, C_{44}Mab-1 (IgG_1, kappa) by CBIS method, and evaluated its applications, including flow cytometry, western blotting, and immunohistochemical analyses of oral squamous cell carcinoma and colorectal adenocarcinomas.

2. Materials and Methods

2.1. Cell Lines

COLO201 (a human colorectal cancer cell line), P3X63Ag8U.1 (P3U1; a mouse multiple myeloma), and Chinese hamster ovary (CHO)-K1 cell lines were obtained from the American Type Culture Collection (ATCC, Manassas, VA, USA). COLO205 (a human colorectal cancer cell line) was obtained from the Cell Resource Center for Biomedical Research Institute of Development, Aging, and Cancer at Tohoku University (Miyagi, Japan). To cultivate these cell lines, we used Roswell Park Memorial Institute (RPMI)-1640 medium (Nacalai Tesque, Inc., Kyoto, Japan), which is supplemented with 10% heat-inactivated fetal bovine serum (FBS; Thermo Fisher Scientific, Inc., Waltham, MA, USA). We

Preprints (www.preprints.org) | NOT PEER-REVIEWED | Posted: 22 March 2023 doi:10.20944/preprints202303.0399.v1

further added the antibiotics, including 100 μg/mL streptomycin, 100 U/mL penicillin, and 0.25 μg/mL amphotericin B (Nacalai Tesque, Inc.). All cell lines were grown in a humidified incubator at 37°C with 5% CO_2.

We amplified CD44s cDNA from LN229 cDNA using HotStar HiFidelity Polymerase Kit (Qiagen Inc., Hilden, Germany). We obtained CD44v3–10 ORF from the RIKEN BRC. CD44v3–10 and CD44s cDNAs were cloned into a pCAG-Ble-ssPA16 vector, which possesses the signal sequence and the N-terminal PA16 tag (GLEGGVAMPGAEDDVV) [24,32-35], which can be detected by an anti-human podoplanin mAb (NZ-1) [36-51]. Using a Neon transfection system (Thermo Fisher Scientific, Inc.), two stable transfectants, such as CHO/CD44v3–10 and CHO/CD44s, were established by introducing pCAG-Ble/PA16-CD44v3–10 and pCAG-Ble/PA16-CD44s into CHO-K1 cells, respectively.

2.2. Production of hybridoma cells

The 6-week-old female BALB/c mice were purchased from CLEA Japan (Tokyo, Japan). Mice were housed under specific pathogen-free conditions. To minimize animal suffering and distress in the laboratory, all mice experiments were performed according to relevant guidelines and regulations. Our animal experiments were approved by the Animal Care and Use Committee of Tohoku University (Permit number: 2019NiA-001). Mice were monitored every day for health during the period of experiments. Mice were intraperitoneally immunized with CHO/CD44v3–10 (1×10^8 cells) with Imject Alum (Thermo Fisher Scientific Inc.) as an adjuvant. We performed additional immunizations of CHO/CD44v3–10 (1×10^8 cells, three times), and performed a booster injection of CHO/CD44v3–10 (1×10^8 cells) 2 days before harvesting the spleen cells. We used polyethylene glycol 1500 (PEG1500; Roche Diagnostics, Indianapolis, IN, USA) to fuse the splenocytes and P3U1 cells. The hybridoma supernatants, which are negative for CHO-K1 cells and positive for CHO/CD44v3–10 cells, were selected using SA3800 Cell Analyzer (Sony Corp. Tokyo, Japan).

2.3. ELISA

Fifty-eight peptides, which cover the extracellular domain of CD44v3–10 [26], were obtained from Sigma-Aldrich Corp. (St. Louis, MO, USA). We immobilized them on Nunc Maxisorp 96-well immunoplates (Thermo Fisher Scientific Inc) at 1 μg/mL for 30 min at 37°C. The palate washing was performed using HydroSpeed Microplate Washer (Tecan, Zürich, Switzerland) with phosphate-buffered saline (PBS) containing 0.05% (*v*/*v*) Tween 20 (PBST; Nacalai Tesque, Inc.). After the blocking with 1% (*w*/*v*) bovine serum albumin (BSA) in PBST for 30 min at 37°C, C_{44}Mab-1 (10 μg/mL) was added to each well. Then, the wells were further incubated with anti-mouse immunoglobulins peroxidase-conjugate (1:2000 diluted; Agilent Technologies Inc., Santa Clara, CA, USA) for 30 min at 37°C. One-Step Ultra TMB (Thermo Fisher Scientific Inc.) was used for enzymatic reactions. An iMark microplate reader (Bio-Rad Laboratories, Inc., Berkeley, CA, USA) was used to mesure the optical density at 655 nm.

2.4. Flow Cytometry

CHO/CD44v3–10 and CHO-K1 cells were prepared using 0.25% trypsin and 1 mM ethylenediamine tetraacetic acid (EDTA; Nacalai Tesque, Inc.). COLO201 and COLO205 were obtained by pipetting. The cells were incubated with C_{44}Mab-1, C_{44}Mab-46, or blocking buffer (0.1% BSA in PBS; control) for 30 min at 4°C. Then, the cells were treated with anti-mouse IgG conjugated with Alexa Fluor 488 (1:2000; Cell Signaling Technology, Inc.) for 30 min at 4°C. Fluorescence data were collected and analyzed using the SA3800 Cell Analyzer and SA3800 software (ver. 2.05, Sony Corp.), respectively.

2.5. Determination of Apparent Dissociation Constant (K_D) by Flow Cytometry

Serially diluted C_{44}Mab-1 was suspended with CHO/CD44v3–10, COLO201, and COLO205 cells. Then, those cells were treated with anti-mouse IgG conjugated with Alexa

Preprints (www.preprints.org) | NOT PEER-REVIEWED | Posted: 22 March 2023 doi:10.20944/preprints202303.0399.v1

Fluor 488 (1:200). Fluorescence data were collected and analyzed as indicated above. GraphPad Prism 8 (the fitting binding isotherms to built-in one-site binding models; GraphPad Software, Inc., La Jolla, CA, USA) was used to determine the apparent dissociation constant (K_D).

2.6. Western Blot Analysis

The 10 μg of cell lysates were subjected to SDS-polyacrylamide gel for electrophoresis using polyacrylamide gels (5–20%; FUJIFILM Wako Pure Chemical Corporation, Osaka, Japan) and electrotransferred onto polyvinylidene difluoride (PVDF) membranes (Merck KGaA, Darmstadt, Germany). The blocking was performed using 4% skim milk (Nacalai Tesque, Inc.) in PBST. The membranes were incubated with 10 μg/mL of C$_{44}$Mab-1, 10 μg/mL of C$_{44}$Mab-46, or 1 μg/mL of an anti-isocitrate dehydrogenase 1 (IDH1; RcMab-1; rat IgG$_{2a}$) [52,53], and then incubated with peroxidase-conjugated anti-mouse immunoglobulins (diluted 1:1000; Agilent Technologies, Inc.) or peroxidase-conjugated anti-rat immunoglobulins (diluted 1:10000; Sigma-Aldrich Corp.). Finally, the signals were enhanced using a chemiluminescence reagent, ImmunoStar LD (FUJIFILM Wako Pure Chemical Corporation), and were detected by a Sayaca-Imager (DRC Co. Ltd., Tokyo, Japan).

2.7. Immunohistochemical Analysis

The formalin-fixed paraffin-embedded (FFPE) oral SCC tissues were obtained as described previously [54]. We purchased a colorectal carcinoma tissue array (CO483a) from US Biomax Inc. (Rockville, MD, USA). The sections were autoclaved in EnVision FLEX Target Retrieval Solution High pH (Agilent Technologies, Inc.) for 20 min. After blocking with SuperBlock T20 (Thermo Fisher Scientific, Inc.), we incubated the tissue sections with C$_{44}$Mab-1 (1 μg/mL) and C$_{44}$Mab-46 (1 μg/mL) for 1 h, and treated with the EnVision+ Kit for mouse (Agilent Technologies Inc.) for 30 min at room temperature. The chromogenic reaction was conducted using 3,3′-diaminobenzidine tetrahydrochloride (DAB; Agilent Technologies Inc.). The counterstaining were performed using hematoxylin (FUJIFILM Wako Pure Chemical Corporation). To examine the sections and obtain images, we used Leica DMD108 (Leica Microsystems GmbH, Wetzlar, Germany).

3. Results

2.1. Establishment of an Anti-CD44v9 mAb, C$_{44}$Mab-1

In the CBIS method, we prepared the CD44v3–10-overexpressed CHO-K1 cells (CHO/CD44v3–10) as an immunogen. As shown in Figure 1, mice were immunized with CHO/CD44v3–10 cells, and hybridomas were produced and seeded into 96-well plates. Then, the supernatants, which were positive to CHO/CD44v3–10 cells and negative to CHO-K1, were selected by high throughput screening using flow cytometry. After cloning by the limiting dilution, anti-CD44 mAb-producing clones were finally established. We next performed the ELISA to determine the epitope of each mAb. Among them, C$_{44}$Mab-1 (IgG$_1$, kappa) was shown to recognize the CD44p471–490 peptide (STSHEGLEEDKDHPTTSTLT), which is corresponding to variant 9-encoded sequence (Supplementary Table S1). In contrast, C$_{44}$Mab-1 never recognized other CD44v3–10 extracellular regions. These results indicated that C$_{44}$Mab-1 specifically recognizes the CD44 variant 9-encoded sequence.

Preprints (www.preprints.org) | NOT PEER-REVIEWED | Posted: 22 March 2023 doi:10.20944/preprints202303.0399.v1

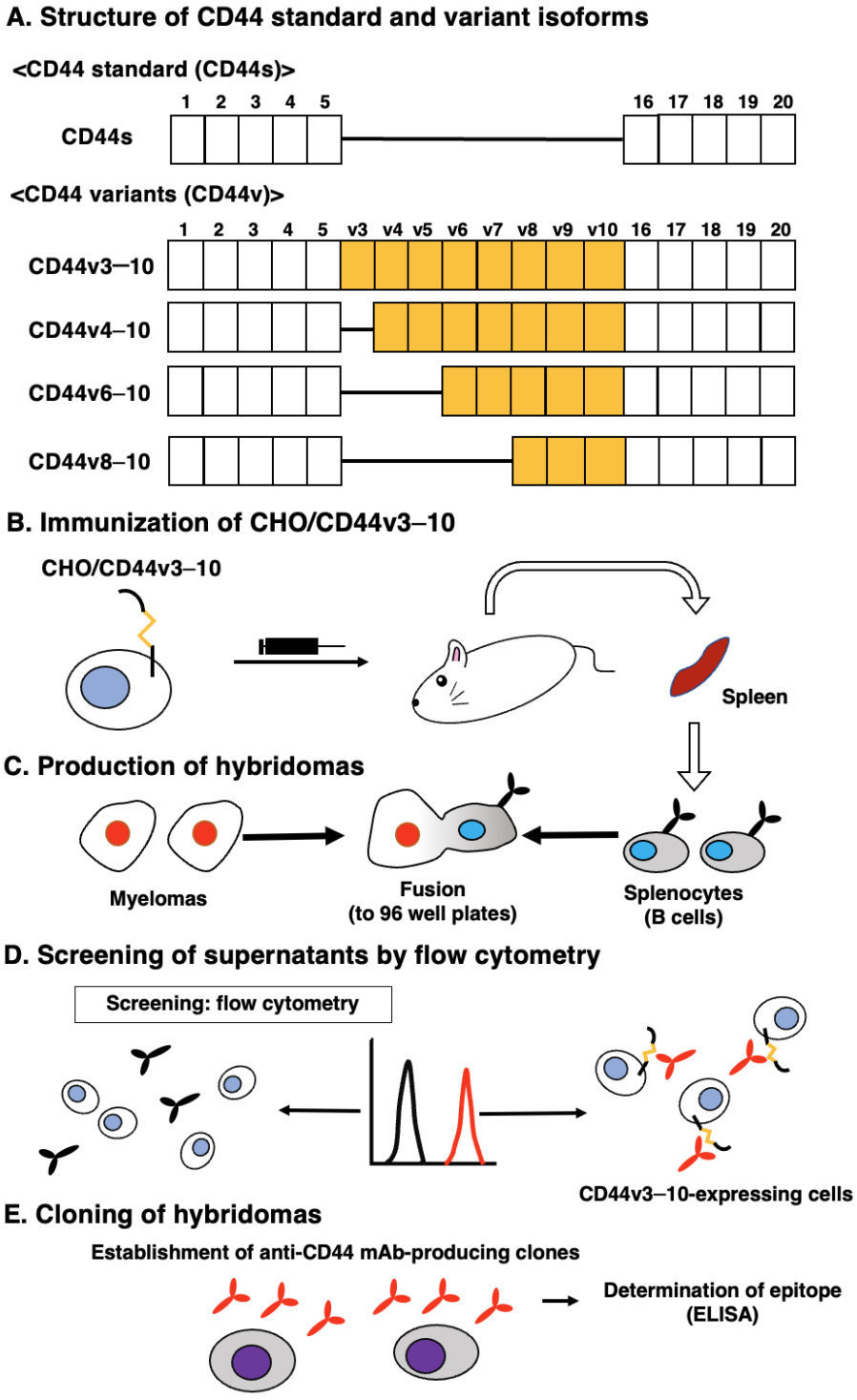

Figure 1. A schematic representation of ant-human CD44 mAbs production. **(A)** Structure of CD44. The CD44s mRNA is assembled by the first five (1 to 5) and the last five (16 to 20) exons, and translates CD44s. The mRNAs of CD44 variant are produced by the alternative splicing of middle variant exons, and translate multiple CD44v such as CD44v3–10, CD44v4–10, CD44v6–10, and CD44v8–10. **(B)** CHO/CD44v3–10 cells were intraperitoneally injected into BALB/c mice. **(C)** Hybridomas were produced by fusion of the splenocytes and P3U1 cells **(D)** The screening was performed by flow cytometry using CHO/CD44v3–10 and parental CHO-K1 cells. **(E)** After cloning and additional screening, a clone C$_{44}$Mab-1 (IgG$_1$, kappa) was established. Furthermore, we used peptides which cover the extracellular domain of CD44v3–10 (Supplementary Table S1), and determined the binding epitopes of each mAbs by enzyme-linked immunosorbent assay (ELISA).

2.2. Flow Cytometric Analysis of C$_{44}$Mab-1 to CD44-Expressing Cells

Preprints (www.preprints.org) | NOT PEER-REVIEWED | Posted: 22 March 2023 doi:10.20944/preprints202303.0399.v1

We next investigated the reactivity of C44Mab-1 against CHO/CD44v3–10 and CHO/CD44s cells by flow cytometry. C44Mab-1 recognized CHO/CD44v3–10 cells in a dose-dependent manner (Figure 2A). In contrast, C44Mab-1 never recognized CHO/CD44s (Figure 2B) nor CHO-K1 (Figure 2C) cells. We confirmed that a pan-CD44 mAb, C44Mab-46 [25], recognized the CHO/CD44s cells (Supplemental Figure S1). Furthermore, C44Mab-1 could recognize endogenous CD44v9 in both COLO201 (Figure 2D) and COLO205 (Figure 2E) cells in a dose-dependent manner.

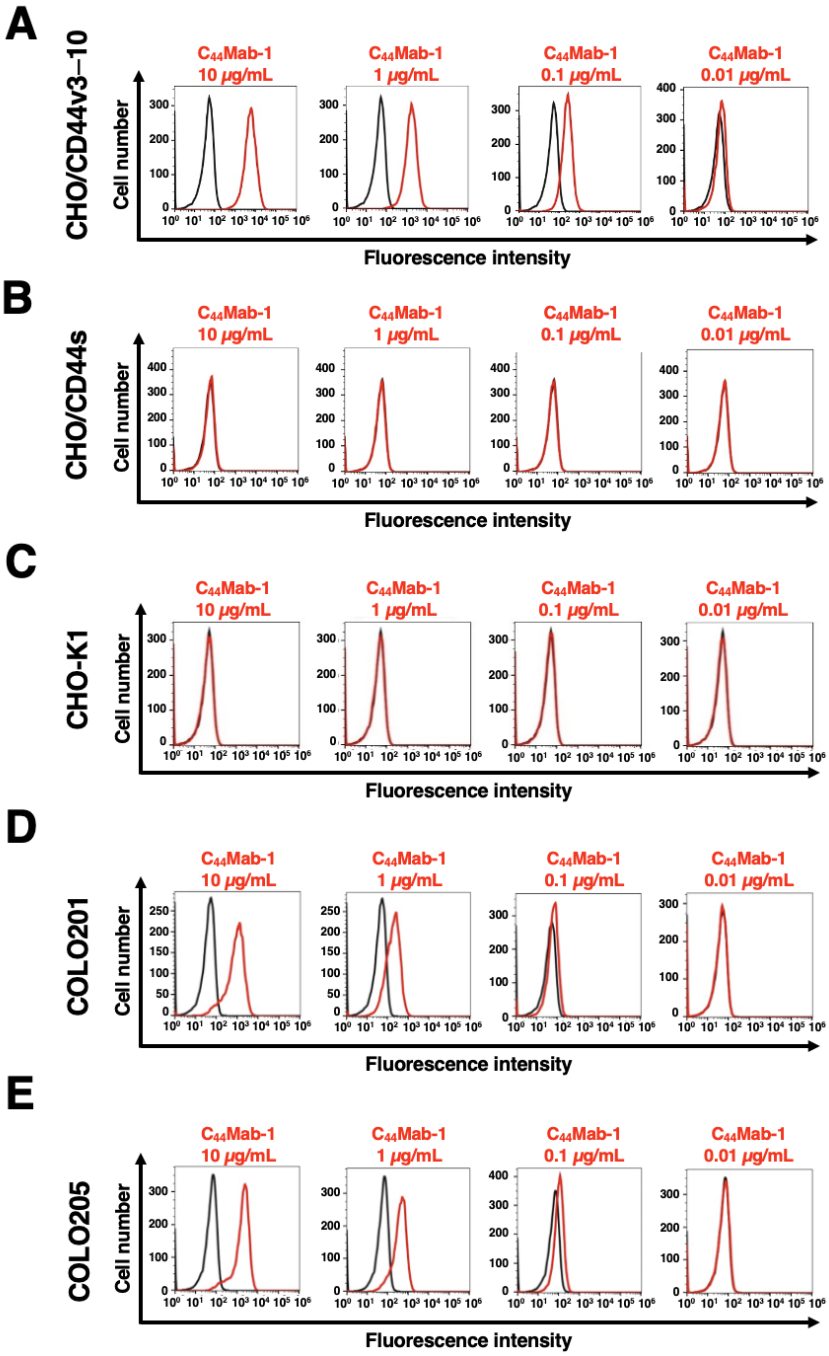

Figure 2. Flow cytometry using C44Mab-1. CHO/CD44v3–10 (**A**), CHO/CD44s (**B**), CHO-K1 (**C**), COLO201 (**D**), and COLO205 (**E**) were treated with 0.01–10 μg/mL of C44Mab-1, followed by treatment with Alexa Fluor 488-conjugated anti-mouse IgG (Red line). The black line represents the negative control (blocking buffer).

We next performed the flow cytometry-based measurement of the apparent binding affinity of C44Mab-1 to CHO/CD44v3–10, COLO201, and COLO205 cells. As shown in

Preprints (www.preprints.org) | NOT PEER-REVIEWED | Posted: 22 March 2023 doi:10.20944/preprints202303.0399.v1

Figure 3, the dissociation constant (K_D) of C44Mab-1 for CHO/CD44v3–10, COLO201, and COLO205 was 2.5×10^{-8} M, 3.3×10^{-8} M, and 6.5×10^{-8} M, respectively. Results indicated that C44Mab-1 possesses the moderate binding affinity for CD44v3–10 or endogenous CD44v9-expressing cells.

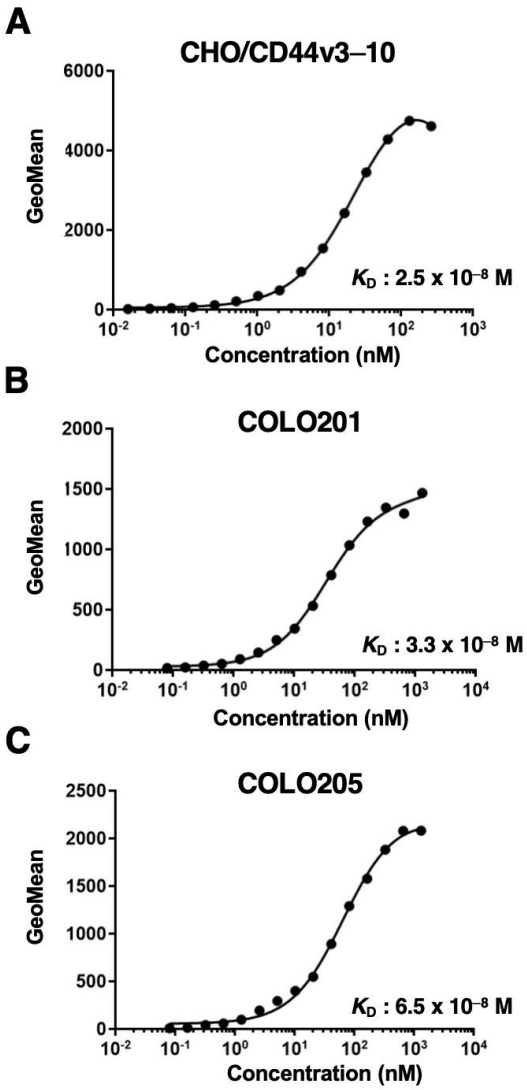

Figure 3. The determination of the the binding affinity of C44Mab-1. Serially diluted C44Mab-1 at indicated concentrations were treated with CHO/CD44v3–10 (**A**), COLO201 (**B**), and COLO205 (**C**). Then, cells were treated with anti-mouse IgG conjugated with Alexa Fluor 488. Fluorescence data were collected, followed by the calculation of the apparent dissociation constant (K_D) by GraphPad PRISM 8.

2.3. Western Blot Analysis

We next performed western blot analysis to assess the sensitivity of C44Mab-1. Total cell lysates of CHO-K1, CHO/CD44s, and CHO/CD44v3–10 were analyzed. As shown in Figure 4, C44Mab-1 detected CD44v3–10 as more than 180-kDa and ~75 kDa bands mainly. However, C44Mab-1 never detect any bands from lysates of CHO/CD44s and CHO-K1 cells (Figure 4A). An anti-pan-CD44 mAb, C44Mab-46, recognized CD44s (~75 kDa) and CD44v3–10 (>180 kDa) bands in the lysates of CHO/CD44s and CHO/CD44v3–10, respectively (Figure 4B). These results indicated that C44Mab-1 is able to detect exogenous CD44v3–10.

Preprints (www.preprints.org) | NOT PEER-REVIEWED | Posted: 22 March 2023 doi:10.20944/preprints202303.0399.v1

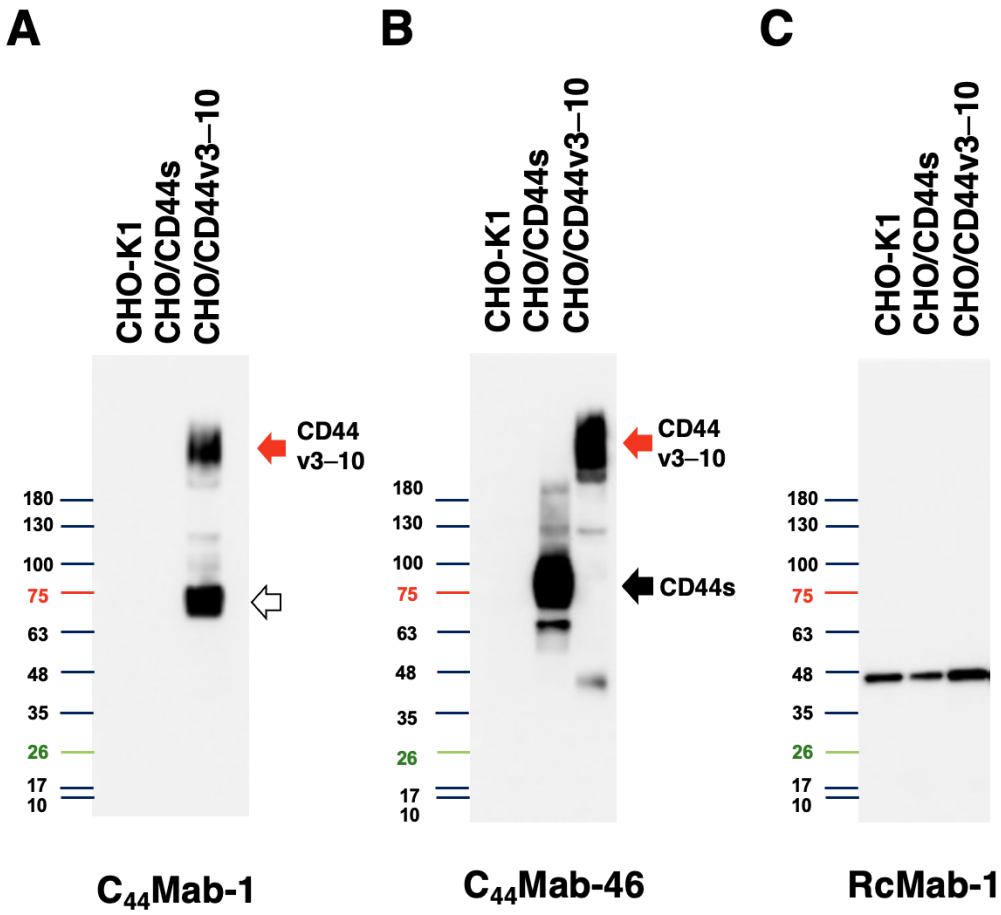

Figure 4. Western blot analysis by C44Mab-1. The total cell lysates (10 μg of protein) were separated and transferred onto polyvinylidene difluoride (PVDF) membranes. The membranes were incubated with 10 μg/mL of C44Mab-1 (**A**), 10 μg/mL of C44Mab-46 (**B**), or 1 μg/mL of RcMab-1 (**C**), followed by incubation with peroxidase-conjugated anti-mouse (for C44Mab-1 and C44Mab-46) or anti-rat (for RcMab-1) immunoglobulins. The red arrows indicate the CD44v3–10 (>180 kDa). The black arrow indicates the CD44s (~75 kDa). The white arrow indicates lower molecular weight band recognized by C44Mab-1 in CHO/CD44v3–10 lysate (~75 kDa).

2.4. Immunohistochemical Analysis using C44Mab-1 against Tumor Tissues

We next examined whether C44Mab-1 could be used for immunohistochemical analyses using FFPE sections. We first examined the reactivity of C44Mab-1 and C44Mab-46 in an oral SCC tissue. As shown in Supplementary Figure S2, C44Mab-1 exhibited a clear membranous staining, and was able to clearly distinguish tumor cells from stromal tissues. In contrast, C44Mab-46 stained the both.

We then investigated the reactivity of C44Mab-1 and C44Mab-46 in the CRC tissue array. C44Mab-1 showed the strong membranous and cytoplasmic staining throughout CRC cells (Figure 5A). C44Mab-46 similarly stained the CRC cells (Figure 5B). In some CRC tissues, both C44Mab-1 and C44Mab-46 stained the basolateral surface of CRC cells (Figure 5C and D). In contrast, both C44Mab-1 and C44Mab-46 never stained CRC cells in some CRC tissues (Figure 5E and F). In addition, stromal staining by C44Mab-46 was also observed in several tumor tissues (Figure 5F). In normal colon epithelium, epithelial cells were rarely stained byC44Mab-1 (Figure 5G). In contrast, C44Mab-46 mainly stained stromal tissues in normal colon epithelium (Figure 5H).

We summarized the data of immunohistochemical analyses in Table 1; C44Mab-1 stained 16 out of 40 cases (40 %) in CRC. These results indicated that C44Mab-1 is useful for immunohistochemical analysis of FFPE tumor sections.

Preprints (www.preprints.org) | NOT PEER-REVIEWED | Posted: 22 March 2023 doi:10.20944/preprints202303.0399.v1

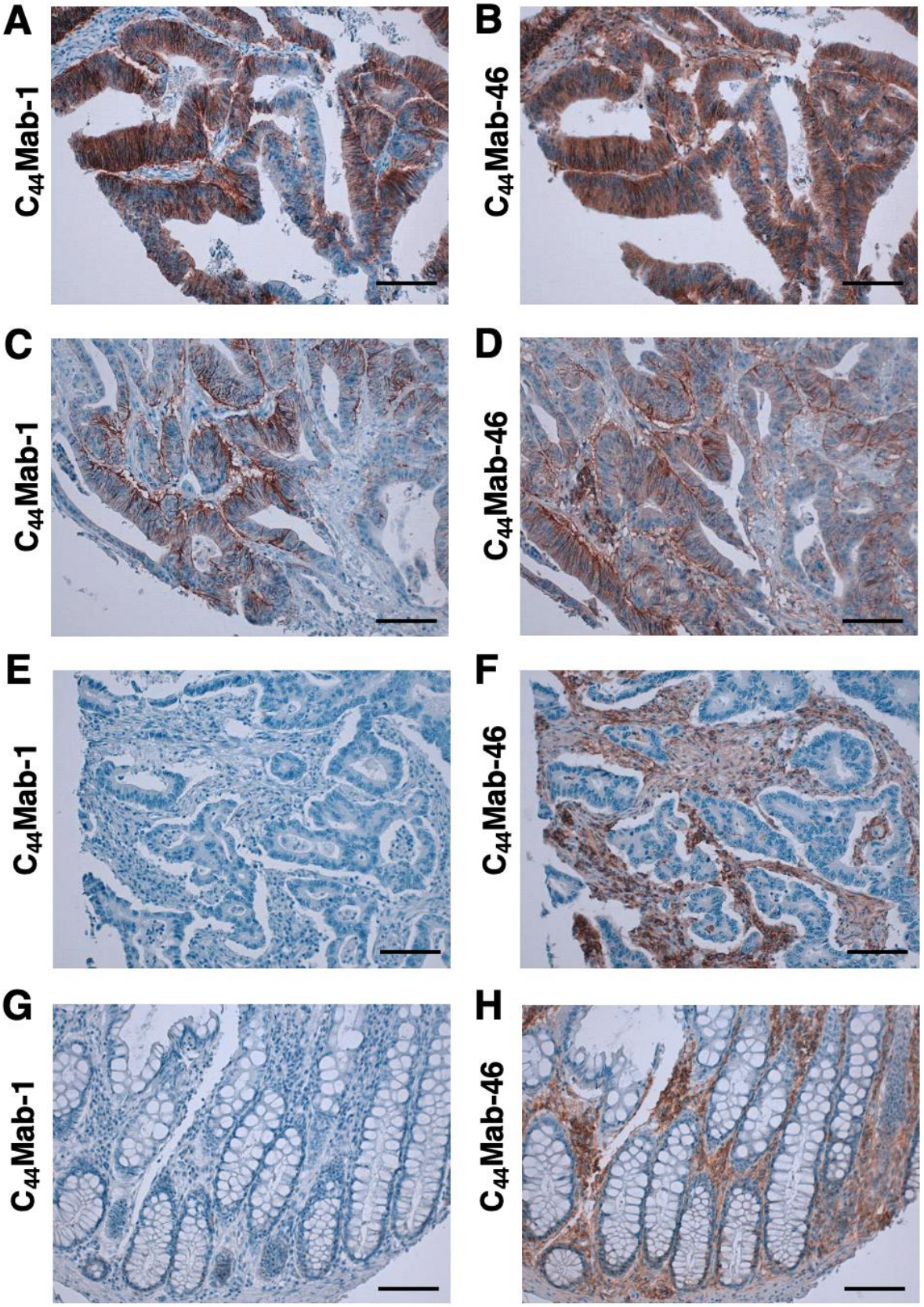

Figure 5. Immunohistochemical analysis using C44Mab1 and C44Mab-46 against CRC tissues. After antigen retrieval, serial sections of CRC tissue arrays (CO483a) were incubated with 1 μg/mL of C44Mab-1 or C44Mab-46 followed by treatment with the Envision+ kit. The color was developed using 3,3'-diaminobenzidine tetrahydrochloride (DAB), and the sections were counterstained with hematoxylin. Scale bar = 100 μm. (**A–F**) CRC; (**G, H**) normal colon epithelium.

Preprints (www.preprints.org) | NOT PEER-REVIEWED | Posted: 22 March 2023 doi:10.20944/preprints202303.0399.v1

Table 1. Immunohistochemical analysis using C44Mab-1 against colorectal carcinoma tissue array.

No	Age	Sex	Organ	Pathology diagnosis	Grade	Stage	Type	C44Mab-1	C44Mab-46
1	67	M	Colon	Adenocarcinoma	1	-	Malignant	+	+
2	48	M	Colon	Adenocarcinoma	1	IIA	Malignant	-	-
3	58	M	Colon	Adenocarcinoma	1--2	IIA	Malignant	+	+
4	75	M	Colon	Adenocarcinoma	1	IV	Malignant	-	++
5	86	M	Colon	Adenocarcinoma	2	II	Malignant	-	+
6	55	M	Colon	Adenocarcinoma	2	IIIC	Malignant	-	-
7	38	M	Colon	Adenocarcinoma	1	I	Malignant	-	++
8	52	M	Colon	Adenocarcinoma	1	IIIB	Malignant	+	-
9	46	M	Colon	Adenocarcinoma	2	IIIB	Malignant	++	+
10	61	M	Colon	Mucinous adenocarcinoma	2	IIIB	Malignant	+	++
11	55	M	Colon	Mucinous adenocarcinoma with necrosis	2	IIA	Malignant	-	++
12	55	M	Colon	Adenocarcinoma	1	IIIB	Malignant	+	-
13	44	M	Colon	Adenocarcinoma	1	-	Malignant	-	-
14	31	M	Colon	Adenocarcinoma	2	IIIB	Malignant	-	+
15	74	F	Colon	Adenocarcinoma	2	IIIB	Malignant	+	+
16	61	M	Colon	Adenocarcinoma	2	II	Malignant	++	++
17	45	M	Colon	Adenocarcinoma	2	III	Malignant	+	+
18	58	M	Colon	Adenocarcinoma	2	IIIB	Malignant	-	++
19	58	M	Colon	Adenocarcinoma	2	IIA	Malignant	+++	+++
20	69	M	Colon	Adenocarcinoma	3	-	Malignant	-	-
21	64	F	Colon	Adenocarcinoma	2	IIIC	Malignant	++	++
22	82	M	Colon	Adenocarcinoma	2	IIIB	Malignant	-	-
23	34	M	Colon	Adenocarcinoma	2	IIIB	Malignant	++	++
24	50	F	Colon	Adenocarcinoma	2	IIB	Malignant	-	-
25	34	F	Colon	Adenocarcinoma	1	IIB	Malignant	-	+
26	52	F	Colon	Adenocarcinoma	2	IIA	Malignant	-	+
27	53	F	Colon	Adenocarcinoma	2	IIIB	Malignant	-	-
28	58	F	Colon	Adenocarcinoma	2	I	Malignant	-	+
29	59	F	Colon	Adenocarcinoma	2	IIA	Malignant	++	++
30	67	M	Colon	Adenocarcinoma	2	IIIB	Malignant	-	++
31	31	M	Colon	Adenocarcinoma	2	IIIB	Malignant	+++	+++
32	54	F	Colon	Adenocarcinoma	2	IIB	Malignant	-	+
33	54	F	Colon	Adenocarcinoma	2	IIIB	Malignant	-	-
34	62	M	Colon	Adenocarcinoma	2	-	Malignant	-	+
35	67	F	Colon	Adenocarcinoma	2	-	Malignant	+	-
36	52	F	Colon	Adenocarcinoma	2	IIA	Malignant	-	-
37	52	F	Colon	Adenocarcinoma	3	IIIB	Malignant	-	-
38	75	M	Colon	Adenocarcinoma	2	-	Malignant	-	-
39	57	F	Colon	Adenocarcinoma	2	IIB	Malignant	+	+++
40	38	M	Colon	Mucinous adenocarcinoma	3	I	Malignant	-	-

4. Discussion

Using the CBIS method, we developed C44Mab-1 (Figure 1), and determined its epitope as variant 9 encoded region by ELISA (Supplementary Table S1). Then, we showed the multiple applications of C44Mab-1 for flow cytometry (Figures 2 and 3), western blotting (Figure 4), and immunohistochemistry using OSCC (Supplementary Figure S2) and CRC tissues (Figure 5 and Table 1).

 doi:10.20944/preprints202303.0399.v1

Ishimoto *et al.* [22] demonstrated that CD44v interacts with xCT, a glutamate-cystine transporter, and regulates the level of reduced glutathione (GSH) in gastric cancer cells. As a result, CD44v contributes to the reduction of intracellular ROS. The knockdown of CD44 reduced the cell surface expression of xCT and suppressed tumor growth in a mouse gastric cancer model. Furthermore, they showed that the v8–10 region of CD44v is required for the specific interaction between CD44v and xCT, and CD44v8–10 (S301A), an *N*-linked glycosylation site mutant, failed to interact with xCT. These results showed an important function for CD44v in the regulation of ROS defense and tumor growth.

Ishimoto *et al.* [22] also established a rat mAb (clone RV3) against CD44v8–10 by immunizing CD44v8–10-expressed RH7777 cells. The epitope of the mAb was determined as a variant 9-encoded region using the recombinant CD44v9 protein by ELISA. RV3 was mainly used in immunohistochemistry and revealed a predictive marker for recurrence of gastric [55] and urothelial [56] cancers, predicting survival outcome in hepatocellular carcinomas [57], and an indicator for identifying a cisplatin-resistant population in urothelial cancers [58]. Therefore, CD44v9 is a critical biomarker to evaluate the malignancy and prognosis of tumors. Furthermore, sulfasalazine, an xCT inhibitor, was shown to suppress the survival of CD44v9-positive CSCs both *in vitro* [59-61] and *in vivo* [62]. A dose-escalation clinical study in patients with advanced gastric cancers revealed that sulfasalazine reduced the population of CD44v9-positive cells in tumors [63], suggesting that CD44v9 is a biomarker for patient selection and efficacy of xCT inhibitors.

As mentioned above, RV3 recognized the recombinant CD44v9 protein by ELISA. Therefore, RV3 is thought to recognize the peptide or glycopeptide structure of CD44v9. However, the detailed binding epitope of RV3 has not been determined. As shown in Supplementary Table S1, C$_{44}$Mab-1 recognized a synthetic peptide (CD44p471–490; STSHEGLEEDKDHPTTSTLT), which possesses multiple predicted and confirmed *O*-glycan sites [64]. As shown in Figure 4A, C$_{44}$Mab-1 recognized a ~75kDa band in CHO/CD44v3–10 lysate, which is approximately identical to predicted molecular weight of CD44v3–10 from the amino acid length. Therefore, C$_{44}$Mab-1 could recognize CD44v3–10 regardless of the glycosylation. The detailed epitope mapping and the influence of the glycosylation on C$_{44}$Mab-1 recognition should be investigated in the future study.

By large-scale genomic analyses, CRCs are classified into 4 subtypes, including microsatellite instability immune, canonical, metabolic, and mesenchymal types [65]. Since the CD44v9 was upregulated in 40% of CRC tissues (Figure 5 and Table 1), the relationship to the subtypes should be determined. Additionally, the mechanism of CD44v9 upregulation including the transcription and the v9 inclusion by alternative splicing should be investigated. Wielenga *et al.* [66] demonstrated that CD44 is a target gene of Wnt/β-catenin in mice intestinal tumor model, suggesting that β-catenin signaling pathway could upregulate CD44 transcription. However, the mechanism of the variant 9 inclusion during the CRC development remains to be determined.

In immunohistochemical analysis, we observed CD44v9 expression throughout CRC cells (Figure 5A) and on the basolateral surface of CRC cells (Figure 5C). The basolateral expression of CD44 was previously observed, and shown to be co-localized with HA [67], EpCAM-Claudin-7 complex [68], and Annexin II [69]. Therefore, the basolateral expression of CD44 may function to promote HA/adhesion-mediated signal transduction and contribute CRC tumorigenesis.

Clinical trials of anti-pan CD44 and CD44v6 mAbs have been conducted [70]. RG7356, an anti-pan CD44 mAb, exhibited an acceptable safety profile. However, the trial was terminated because of no clinical and dose-response relationship with RG7356 [71]. Clinical trials of an antibody-drug conjugate (ADC), an anti-CD44v6 mAb bivatuzumab−mertansine, were conducted. However, it failed due to the high toxicity to skin [72,73]. The anti-CD44v6 mAb is further developed to chimeric antigen receptor T (CAR-T) cell therapy. The CD44v6 CAR-T showed antitumor effects against primary human multiple myeloma and acute myeloid leukemia [74]. Furthermore, the CD44v6 CAR-T also suppressed the xenograft tumor growth of lung and ovarian carcinomas [75], which is expected for the application against solid tumors. Although CD44v9 is rarely detected

 doi:10.20944/preprints202303.0399.v1

in normal colon epithelium by C44Mab-1, CD44v9 could be detected in other normal tissues including oral squamous epithelium (Supplementary Figure S2). For the development of therapeutic use of C44Mab-1, further investigations are required to reduce the toxicity to above tissues.

Because anti-CD44 mAbs could have side effects by affecting normal tissues, the clinical applications of anti-CD44 mAbs are still limited We previously developed PDPN-targeting cancer-specific mAbs (CasMabs) [76-79] and podocalyxin-targeting CasMabs [80], which are currently applied to CAR-T therapy in mice models [46,81,82]. These CasMabs recognize cancer specific aberrant glycosylation of the target proteins [83]. It is worthwhile to establish cancer-specific anti-CD44 mAbs using the CasMab method. Anti-CD44 CasMab production can be applicable as a basis for designing and optimizing potent immunotherapy modalities, including ADCs and CAR-T therapies.

Supplementary Materials: The following supporting information can be downloaded at the website of this paper posted on Preprints.org.

Author Contributions: M.T., T.T. and T.A. performed the experiments. M.K.K. and Y.K. designed the experiments. M.T. and H.S. analyzed the data. M.T., H.S. and Y.K. wrote the manuscript. All authors have read and agreed to the published version of the manuscript.

Funding: This research was supported in part by Japan Agency for Medical Research and Development (AMED) under Grant Numbers: JP22ama121008 (to Y.K.), JP22am0401013 (to Y.K.), JP22bm1004001 (to Y.K.), JP22ck0106730 (to Y.K.), and JP21am0101078 (to Y.K.), and by the Japan Society for the Promotion of Science (JSPS) Grants-in-Aid for Scientific Research (KAKENHI) grant nos. 21K20789 (to T.T.), 22K06995 (to H.S.), 21K07168 (to M.K.K.), and 22K07224 (to Y.K.).

Institutional Review Board Statement: The animal study protocol was approved by the Animal Care and Use Committee of Tohoku University (Permit number: 2019NiA-001) for studies involving animals.

Data Availability Statement: All related data and methods are presented in this paper. Additional inquiries should be addressed to the corresponding authors.

Conflicts of Interest: The authors declare no conflicts of interest involving this article.

References

1. Fox, S.B.; Fawcett, J.; Jackson, D.G.; Collins, I.; Gatter, K.C.; Harris, A.L.; Gearing, A.; Simmons, D.L. Normal human tissues, in addition to some tumors, express multiple different CD44 isoforms. *Cancer Res* **1994**, *54*, 4539-4546.
2. Ponta, H.; Sherman, L.; Herrlich, P.A. CD44: from adhesion molecules to signalling regulators. *Nat Rev Mol Cell Biol* **2003**, *4*, 33-45, doi:10.1038/nrm1004.
3. Yan, Y.; Zuo, X.; Wei, D. Concise Review: Emerging Role of CD44 in Cancer Stem Cells: A Promising Biomarker and Therapeutic Target. *Stem Cells Transl Med* **2015**, *4*, 1033-1043, doi:10.5966/sctm.2015-0048.
4. Chen, C.; Zhao, S.; Karnad, A.; Freeman, J.W. The biology and role of CD44 in cancer progression: therapeutic implications. *J Hematol Oncol* **2018**, *11*, 64, doi:10.1186/s13045-018-0605-5.
5. Slevin, M.; Krupinski, J.; Gaffney, J.; Matou, S.; West, D.; Delisser, H.; Savani, R.C.; Kumar, S. Hyaluronan-mediated angiogenesis in vascular disease: uncovering RHAMM and CD44 receptor signaling pathways. *Matrix Biol* **2007**, *26*, 58-68, doi:10.1016/j.matbio.2006.08.261.
6. Chen, K.L.; Li, D.; Lu, T.X.; Chang, S.W. Structural Characterization of the CD44 Stem Region for Standard and Cancer-Associated Isoforms. *Int J Mol Sci* **2020**, *21*, doi:10.3390/ijms21010336.
7. Mishra, M.N.; Chandavarkar, V.; Sharma, R.; Bhargava, D. Structure, function and role of CD44 in neoplasia. *J Oral Maxillofac Pathol* **2019**, *23*, 267-272, doi:10.4103/jomfp.JOMFP_246_18.
8. Hassn Mesrati, M.; Syafruddin, S.E.; Mohtar, M.A.; Syahir, A. CD44: A Multifunctional Mediator of Cancer Progression. *Biomolecules* **2021**, *11*, doi:10.3390/biom11121850.

9. Ludwig, N.; Szczepanski, M.J.; Gluszko, A.; Szafarowski, T.; Azambuja, J.H.; Dolg, L.; Gellrich, N.C.; Kampmann, A.; Whiteside, T.L.; Zimmerer, R.M. CD44(+) tumor cells promote early angiogenesis in head and neck squamous cell carcinoma. *Cancer Lett* **2019**, *467*, 85-95, doi:10.1016/j.canlet.2019.10.010.
10. Durko, L.; Wlodarski, W.; Stasikowska-Kanicka, O.; Wagrowska-Danilewicz, M.; Danilewicz, M.; Hogendorf, P.; Strzelczyk, J.; Malecka-Panas, E. Expression and Clinical Significance of Cancer Stem Cell Markers CD24, CD44, and CD133 in Pancreatic Ductal Adenocarcinoma and Chronic Pancreatitis. *Dis Markers* **2017**, *2017*, 3276806, doi:10.1155/2017/3276806.
11. Gzil, A.; Zarębska, I.; Bursiewicz, W.; Antosik, P.; Grzanka, D.; Szylberg, Ł. Markers of pancreatic cancer stem cells and their clinical and therapeutic implications. *Mol Biol Rep* **2019**, *46*, 6629-6645, doi:10.1007/s11033-019-05058-1.
12. Liu, X.; Taftaf, R.; Kawaguchi, M.; Chang, Y.F.; Chen, W.; Entenberg, D.; Zhang, Y.; Gerratana, L.; Huang, S.; Patel, D.B.; et al. Homophilic CD44 Interactions Mediate Tumor Cell Aggregation and Polyclonal Metastasis in Patient-Derived Breast Cancer Models. *Cancer Discov* **2019**, *9*, 96-113, doi:10.1158/2159-8290.Cd-18-0065.
13. Hassn Mesrati, M.; Behrooz, A.B.; A, Y.A.; Syahir, A. Understanding Glioblastoma Biomarkers: Knocking a Mountain with a Hammer. *Cells* **2020**, *9*, doi:10.3390/cells9051236.
14. Wolf, K.J.; Shukla, P.; Springer, K.; Lee, S.; Coombes, J.D.; Choy, C.J.; Kenny, S.J.; Xu, K.; Kumar, S. A mode of cell adhesion and migration facilitated by CD44-dependent microtentacles. *Proc Natl Acad Sci U S A* **2020**, *117*, 11432-11443, doi:10.1073/pnas.1914294117.
15. Li, W.; Qian, L.; Lin, J.; Huang, G.; Hao, N.; Wei, X.; Wang, W.; Liang, J. CD44 regulates prostate cancer proliferation, invasion and migration via PDK1 and PFKFB4. *Oncotarget* **2017**, *8*, 65143-65151, doi:10.18632/oncotarget.17821.
16. Wang, Z.; Tang, Y.; Xie, L.; Huang, A.; Xue, C.; Gu, Z.; Wang, K.; Zong, S. The Prognostic and Clinical Value of CD44 in Colorectal Cancer: A Meta-Analysis. *Front Oncol* **2019**, *9*, 309, doi:10.3389/fonc.2019.00309.
17. Zöller, M. CD44: can a cancer-initiating cell profit from an abundantly expressed molecule? *Nat Rev Cancer* **2011**, *11*, 254-267, doi:10.1038/nrc3023.
18. Guo, Q.; Yang, C.; Gao, F. The state of CD44 activation in cancer progression and therapeutic targeting. *Febs j* **2021**, doi:10.1111/febs.16179.
19. Morath, I.; Hartmann, T.N.; Orian-Rousseau, V. CD44: More than a mere stem cell marker. *Int J Biochem Cell Biol* **2016**, *81*, 166-173, doi:10.1016/j.biocel.2016.09.009.
20. Bennett, K.L.; Jackson, D.G.; Simon, J.C.; Tanczos, E.; Peach, R.; Modrell, B.; Stamenkovic, I.; Plowman, G.; Aruffo, A. CD44 isoforms containing exon V3 are responsible for the presentation of heparin-binding growth factor. *J Cell Biol* **1995**, *128*, 687-698, doi:10.1083/jcb.128.4.687.
21. Orian-Rousseau, V.; Chen, L.; Sleeman, J.P.; Herrlich, P.; Ponta, H. CD44 is required for two consecutive steps in HGF/c-Met signaling. *Genes Dev* **2002**, *16*, 3074-3086, doi:10.1101/gad.242602.
22. Ishimoto, T.; Nagano, O.; Yae, T.; Tamada, M.; Motohara, T.; Oshima, H.; Oshima, M.; Ikeda, T.; Asaba, R.; Yagi, H.; et al. CD44 variant regulates redox status in cancer cells by stabilizing the xCT subunit of system xc(-) and thereby promotes tumor growth. *Cancer Cell* **2011**, *19*, 387-400, doi:10.1016/j.ccr.2011.01.038.
23. Kagami, T.; Yamade, M.; Suzuki, T.; Uotani, T.; Tani, S.; Hamaya, Y.; Iwaizumi, M.; Osawa, S.; Sugimoto, K.; Baba, S.; et al. High expression level of CD44v8-10 in cancer stem-like cells is associated with poor prognosis in esophageal squamous cell carcinoma patients treated with chemoradiotherapy. *Oncotarget* **2018**, *9*, 34876-34888, doi:10.18632/oncotarget.26172.
24. Yamada, S.; Itai, S.; Nakamura, T.; Yanaka, M.; Kaneko, M.K.; Kato, Y. Detection of high CD44 expression in oral cancers using the novel monoclonal antibody, C(44)Mab-5. *Biochem Biophys Rep* **2018**, *14*, 64-68, doi:10.1016/j.bbrep.2018.03.007.
25. Goto, N.; Suzuki, H.; Tanaka, T.; Asano, T.; Kaneko, M.K.; Kato, Y. Development of a Novel Anti-CD44 Monoclonal Antibody for Multiple Applications against Esophageal Squamous Cell Carcinomas. *Int J Mol Sci* **2022**, *23*, doi:10.3390/ijms23105535.

26. Takei, J.; Asano, T.; Suzuki, H.; Kaneko, M.K.; Kato, Y. Epitope Mapping of the Anti-CD44 Monoclonal Antibody (C44Mab-46) Using Alanine-Scanning Mutagenesis and Surface Plasmon Resonance. *Monoclon Antib Immunodiagn Immunother* **2021**, *40*, 219-226, doi:10.1089/mab.2021.0028.
27. Asano, T.; Kaneko, M.K.; Takei, J.; Tateyama, N.; Kato, Y. Epitope Mapping of the Anti-CD44 Monoclonal Antibody (C44Mab-46) Using the REMAP Method. *Monoclon Antib Immunodiagn Immunother* **2021**, *40*, 156-161, doi:10.1089/mab.2021.0012.
28. Asano, T.; Kaneko, M.K.; Kato, Y. Development of a Novel Epitope Mapping System: RIEDL Insertion for Epitope Mapping Method. *Monoclon Antib Immunodiagn Immunother* **2021**, *40*, 162-167, doi:10.1089/mab.2021.0023.
29. Takei, J.; Kaneko, M.K.; Ohishi, T.; Hosono, H.; Nakamura, T.; Yanaka, M.; Sano, M.; Asano, T.; Sayama, Y.; Kawada, M.; et al. A defucosylated antiCD44 monoclonal antibody 5mG2af exerts antitumor effects in mouse xenograft models of oral squamous cell carcinoma. *Oncol Rep* **2020**, *44*, 1949-1960, doi:10.3892/or.2020.7735.
30. Suzuki, H.; Tanaka, T.; Goto, N.; Kaneko, M.K.; Kato, Y. Development of a Novel Anti-CD44 Variant 4 Monoclonal Antibody C44Mab-108 for Immunohistochemistry. *Curr Issues Mol Biol* **2023**, *45*, 1875-1888, doi:10.3390/cimb45030121.
31. Ejima, R.; Suzuki, H.; Tanaka, T.; Asano, T.; Kaneko, M.K.; Kato, Y. Development of a Novel Anti-CD44 Variant 6 Monoclonal Antibody C(44)Mab-9 for Multiple Applications against Colorectal Carcinomas. *Int J Mol Sci* **2023**, *24*, doi:10.3390/ijms24044007.
32. Kato, Y.; Yamada, S.; Furusawa, Y.; Itai, S.; Nakamura, T.; Yanaka, M.; Sano, M.; Harada, H.; Fukui, M.; Kaneko, M.K. PMab-213: A Monoclonal Antibody for Immunohistochemical Analysis Against Pig Podoplanin. *Monoclon Antib Immunodiagn Immunother* **2019**, *38*, 18-24, doi:10.1089/mab.2018.0048.
33. Furusawa, Y.; Yamada, S.; Itai, S.; Sano, M.; Nakamura, T.; Yanaka, M.; Fukui, M.; Harada, H.; Mizuno, T.; Sakai, Y.; et al. PMab-210: A Monoclonal Antibody Against Pig Podoplanin. *Monoclon Antib Immunodiagn Immunother* **2019**, *38*, 30-36, doi:10.1089/mab.2018.0038.
34. Furusawa, Y.; Yamada, S.; Itai, S.; Nakamura, T.; Yanaka, M.; Sano, M.; Harada, H.; Fukui, M.; Kaneko, M.K.; Kato, Y. PMab-219: A monoclonal antibody for the immunohistochemical analysis of horse podoplanin. *Biochem Biophys Rep* **2019**, *18*, 100616, doi:10.1016/j.bbrep.2019.01.009.
35. Furusawa, Y.; Yamada, S.; Itai, S.; Nakamura, T.; Takei, J.; Sano, M.; Harada, H.; Fukui, M.; Kaneko, M.K.; Kato, Y. Establishment of a monoclonal antibody PMab-233 for immunohistochemical analysis against Tasmanian devil podoplanin. *Biochem Biophys Rep* **2019**, *18*, 100631, doi:10.1016/j.bbrep.2019.100631.
36. Kato, Y.; Kaneko, M.K.; Kuno, A.; Uchiyama, N.; Amano, K.; Chiba, Y.; Hasegawa, Y.; Hirabayashi, J.; Narimatsu, H.; Mishima, K.; et al. Inhibition of tumor cell-induced platelet aggregation using a novel anti-podoplanin antibody reacting with its platelet-aggregation-stimulating domain. *Biochem Biophys Res Commun* **2006**, *349*, 1301-1307, doi:10.1016/j.bbrc.2006.08.171.
37. Chalise, L.; Kato, A.; Ohno, M.; Maeda, S.; Yamamichi, A.; Kuramitsu, S.; Shiina, S.; Takahashi, H.; Ozone, S.; Yamaguchi, J.; et al. Efficacy of cancer-specific anti-podoplanin CAR-T cells and oncolytic herpes virus G47Delta combination therapy against glioblastoma. *Mol Ther Oncolytics* **2022**, *26*, 265-274, doi:10.1016/j.omto.2022.07.006.
38. Ishikawa, A.; Waseda, M.; Ishii, T.; Kaneko, M.K.; Kato, Y.; Kaneko, S. Improved anti-solid tumor response by humanized anti-podoplanin chimeric antigen receptor transduced human cytotoxic T cells in an animal model. *Genes Cells* **2022**, *27*, 549-558, doi:10.1111/gtc.12972.
39. Tamura-Sakaguchi, R.; Aruga, R.; Hirose, M.; Ekimoto, T.; Miyake, T.; Hizukuri, Y.; Oi, R.; Kaneko, M.K.; Kato, Y.; Akiyama, Y.; et al. Moving toward generalizable NZ-1 labeling for 3D structure determination with optimized epitope-tag insertion. *Acta Crystallogr D Struct Biol* **2021**, *77*, 645-662, doi:10.1107/S2059798321002527.

40. Kaneko, M.K.; Ohishi, T.; Nakamura, T.; Inoue, H.; Takei, J.; Sano, M.; Asano, T.; Sayama, Y.; Hosono, H.; Suzuki, H.; et al. Development of Core-Fucose-Deficient Humanized and Chimeric Anti-Human Podoplanin Antibodies. *Monoclon Antib Immunodiagn Immunother* **2020**, *39*, 167-174, doi:10.1089/mab.2020.0019.
41. Fujii, Y.; Matsunaga, Y.; Arimori, T.; Kitago, Y.; Ogasawara, S.; Kaneko, M.K.; Kato, Y.; Takagi, J. Tailored placement of a turn-forming PA tag into the structured domain of a protein to probe its conformational state. *J Cell Sci* **2016**, *129*, 1512-1522, doi:10.1242/jcs.176685.
42. Abe, S.; Kaneko, M.K.; Tsuchihashi, Y.; Izumi, T.; Ogasawara, S.; Okada, N.; Sato, C.; Tobiume, M.; Otsuka, K.; Miyamoto, L.; et al. Antitumor effect of novel anti-podoplanin antibody NZ-12 against malignant pleural mesothelioma in an orthotopic xenograft model. *Cancer Sci* **2016**, *107*, 1198-1205, doi:10.1111/cas.12985.
43. Kaneko, M.K.; Abe, S.; Ogasawara, S.; Fujii, Y.; Yamada, S.; Murata, T.; Uchida, H.; Tahara, H.; Nishioka, Y.; Kato, Y. Chimeric Anti-Human Podoplanin Antibody NZ-12 of Lambda Light Chain Exerts Higher Antibody-Dependent Cellular Cytotoxicity and Complement-Dependent Cytotoxicity Compared with NZ-8 of Kappa Light Chain. *Monoclon Antib Immunodiagn Immunother* **2017**, *36*, 25-29, doi:10.1089/mab.2016.0047.
44. Ito, A.; Ohta, M.; Kato, Y.; Inada, S.; Kato, T.; Nakata, S.; Yatabe, Y.; Goto, M.; Kaneda, N.; Kurita, K.; et al. A Real-Time Near-Infrared Fluorescence Imaging Method for the Detection of Oral Cancers in Mice Using an Indocyanine Green-Labeled Podoplanin Antibody. *Technol Cancer Res Treat* **2018**, *17*, 1533033818767936, doi:10.1177/1533033818767936.
45. Tamura, R.; Oi, R.; Akashi, S.; Kaneko, M.K.; Kato, Y.; Nogi, T. Application of the NZ-1 Fab as a crystallization chaperone for PA tag-inserted target proteins. *Protein Sci* **2019**, *28*, 823-836, doi:10.1002/pro.3580.
46. Shiina, S.; Ohno, M.; Ohka, F.; Kuramitsu, S.; Yamamichi, A.; Kato, A.; Motomura, K.; Tanahashi, K.; Yamamoto, T.; Watanabe, R.; et al. CAR T Cells Targeting Podoplanin Reduce Orthotopic Glioblastomas in Mouse Brains. *Cancer Immunol Res* **2016**, *4*, 259-268, doi:10.1158/2326-6066.CIR-15-0060.
47. Kuwata, T.; Yoneda, K.; Mori, M.; Kanayama, M.; Kuroda, K.; Kaneko, M.K.; Kato, Y.; Tanaka, F. Detection of Circulating Tumor Cells (CTCs) in Malignant Pleural Mesothelioma (MPM) with the "Universal" CTC-Chip and An Anti-Podoplanin Antibody NZ-1.2. *Cells* **2020**, *9*, doi:10.3390/cells9040888.
48. Nishinaga, Y.; Sato, K.; Yasui, H.; Taki, S.; Takahashi, K.; Shimizu, M.; Endo, R.; Koike, C.; Kuramoto, N.; Nakamura, S.; et al. Targeted Phototherapy for Malignant Pleural Mesothelioma: Near-Infrared Photoimmunotherapy Targeting Podoplanin. *Cells* **2020**, *9*, doi:10.3390/cells9041019.
49. Fujii, Y.; Kaneko, M.; Neyazaki, M.; Nogi, T.; Kato, Y.; Takagi, J. PA tag: a versatile protein tagging system using a super high affinity antibody against a dodecapeptide derived from human podoplanin. *Protein Expr Purif* **2014**, *95*, 240-247, doi:10.1016/j.pep.2014.01.009.
50. Kato, Y.; Kaneko, M.K.; Kunita, A.; Ito, H.; Kameyama, A.; Ogasawara, S.; Matsuura, N.; Hasegawa, Y.; Suzuki-Inoue, K.; Inoue, O.; et al. Molecular analysis of the pathophysiological binding of the platelet aggregation-inducing factor podoplanin to the C-type lectin-like receptor CLEC-2. *Cancer Sci* **2008**, *99*, 54-61, doi:10.1111/j.1349-7006.2007.00634.x.
51. Kato, Y.; Vaidyanathan, G.; Kaneko, M.K.; Mishima, K.; Srivastava, N.; Chandramohan, V.; Pegram, C.; Keir, S.T.; Kuan, C.T.; Bigner, D.D.; et al. Evaluation of anti-podoplanin rat monoclonal antibody NZ-1 for targeting malignant gliomas. *Nucl Med Biol* **2010**, *37*, 785-794, doi:10.1016/j.nucmedbio.2010.03.010.
52. Kato, Y. Specific monoclonal antibodies against IDH1/2 mutations as diagnostic tools for gliomas. *Brain Tumor Pathol* **2015**, *32*, 3-11, doi:10.1007/s10014-014-0202-4.
53. Ikota, H.; Nobusawa, S.; Arai, H.; Kato, Y.; Ishizawa, K.; Hirose, T.; Yokoo, H. Evaluation of IDH1 status in diffusely infiltrating gliomas by immunohistochemistry using anti-mutant and wild type IDH1 antibodies. *Brain Tumor Pathol* **2015**, *32*, 237-244, doi:10.1007/s10014-015-0222-8.

54. Itai, S.; Ohishi, T.; Kaneko, M.K.; Yamada, S.; Abe, S.; Nakamura, T.; Yanaka, M.; Chang, Y.W.; Ohba, S.I.; Nishioka, Y.; et al. Anti-podocalyxin antibody exerts antitumor effects via antibody-dependent cellular cytotoxicity in mouse xenograft models of oral squamous cell carcinoma. *Oncotarget* **2018**, *9*, 22480-22497, doi:10.18632/oncotarget.25132.
55. Hirata, K.; Suzuki, H.; Imaeda, H.; Matsuzaki, J.; Tsugawa, H.; Nagano, O.; Asakura, K.; Saya, H.; Hibi, T. CD44 variant 9 expression in primary early gastric cancer as a predictive marker for recurrence. *Br J Cancer* **2013**, *109*, 379-386, doi:10.1038/bjc.2013.314.
56. Hagiwara, M.; Kikuchi, E.; Kosaka, T.; Mikami, S.; Saya, H.; Oya, M. Variant isoforms of CD44 expression in upper tract urothelial cancer as a predictive marker for recurrence and mortality. *Urol Oncol* **2016**, *34*, 337.e319-326, doi:10.1016/j.urolonc.2016.03.015.
57. Kakehashi, A.; Ishii, N.; Sugihara, E.; Gi, M.; Saya, H.; Wanibuchi, H. CD44 variant 9 is a potential biomarker of tumor initiating cells predicting survival outcome in hepatitis C virus-positive patients with resected hepatocellular carcinoma. *Cancer Sci* **2016**, *107*, 609-618, doi:10.1111/cas.12908.
58. Hagiwara, M.; Kikuchi, E.; Tanaka, N.; Kosaka, T.; Mikami, S.; Saya, H.; Oya, M. Variant isoforms of CD44 involves acquisition of chemoresistance to cisplatin and has potential as a novel indicator for identifying a cisplatin-resistant population in urothelial cancer. *BMC Cancer* **2018**, *18*, 113, doi:10.1186/s12885-018-3988-3.
59. Seishima, R.; Okabayashi, K.; Nagano, O.; Hasegawa, H.; Tsuruta, M.; Shimoda, M.; Kameyama, K.; Saya, H.; Kitagawa, Y. Sulfasalazine, a therapeutic agent for ulcerative colitis, inhibits the growth of CD44v9(+) cancer stem cells in ulcerative colitis-related cancer. *Clin Res Hepatol Gastroenterol* **2016**, *40*, 487-493, doi:10.1016/j.clinre.2015.11.007.
60. Miyoshi, S.; Tsugawa, H.; Matsuzaki, J.; Hirata, K.; Mori, H.; Saya, H.; Kanai, T.; Suzuki, H. Inhibiting xCT Improves 5-Fluorouracil Resistance of Gastric Cancer Induced by CD44 Variant 9 Expression. *Anticancer Res* **2018**, *38*, 6163-6170, doi:10.21873/anticanres.12969.
61. Tsugawa, H.; Kato, C.; Mori, H.; Matsuzaki, J.; Kameyama, K.; Saya, H.; Hatakeyama, M.; Suematsu, M.; Suzuki, H. Cancer Stem-Cell Marker CD44v9-Positive Cells Arise From Helicobacter pylori-Infected CAPZA1-Overexpressing Cells. *Cell Mol Gastroenterol Hepatol* **2019**, *8*, 319-334, doi:10.1016/j.jcmgh.2019.05.008.
62. Thanee, M.; Padthaisong, S.; Suksawat, M.; Dokduang, H.; Phetcharaburanin, J.; Klanrit, P.; Titapun, A.; Namwat, N.; Wangwiwatsin, A.; Sa-Ngiamwibool, P.; et al. Sulfasalazine modifies metabolic profiles and enhances cisplatin chemosensitivity on cholangiocarcinoma cells in in vitro and in vivo models. *Cancer Metab* **2021**, *9*, 11, doi:10.1186/s40170-021-00249-6.
63. Shitara, K.; Doi, T.; Nagano, O.; Imamura, C.K.; Ozeki, T.; Ishii, Y.; Tsuchihashi, K.; Takahashi, S.; Nakajima, T.E.; Hironaka, S.; et al. Dose-escalation study for the targeting of CD44v(+) cancer stem cells by sulfasalazine in patients with advanced gastric cancer (EPOC1205). *Gastric Cancer* **2017**, *20*, 341-349, doi:10.1007/s10120-016-0610-8.
64. Mereiter, S.; Martins Á, M.; Gomes, C.; Balmaña, M.; Macedo, J.A.; Polom, K.; Roviello, F.; Magalhães, A.; Reis, C.A. O-glycan truncation enhances cancer-related functions of CD44 in gastric cancer. *FEBS Lett* **2019**, *593*, 1675-1689, doi:10.1002/1873-3468.13432.
65. Guinney, J.; Dienstmann, R.; Wang, X.; de Reyniès, A.; Schlicker, A.; Soneson, C.; Marisa, L.; Roepman, P.; Nyamundanda, G.; Angelino, P.; et al. The consensus molecular subtypes of colorectal cancer. *Nat Med* **2015**, *21*, 1350-1356, doi:10.1038/nm.3967.
66. Wielenga, V.J.; Smits, R.; Korinek, V.; Smit, L.; Kielman, M.; Fodde, R.; Clevers, H.; Pals, S.T. Expression of CD44 in Apc and Tcf mutant mice implies regulation by the WNT pathway. *Am J Pathol* **1999**, *154*, 515-523, doi:10.1016/s0002-9440(10)65297-2.
67. Green, S.J.; Tarone, G.; Underhill, C.B. Distribution of hyaluronate and hyaluronate receptors in the adult lung. *J Cell Sci* **1988**, *90 (Pt 1)*, 145-156, doi:10.1242/jcs.90.1.145.

68. Kuhn, S.; Koch, M.; Nübel, T.; Ladwein, M.; Antolovic, D.; Klingbeil, P.; Hildebrand, D.; Moldenhauer, G.; Langbein, L.; Franke, W.W.; et al. A complex of EpCAM, claudin-7, CD44 variant isoforms, and tetraspanins promotes colorectal cancer progression. *Mol Cancer Res* **2007**, *5*, 553-567, doi:10.1158/1541-7786.Mcr-06-0384.
69. Oliferenko, S.; Paiha, K.; Harder, T.; Gerke, V.; Schwärzler, C.; Schwarz, H.; Beug, H.; Günthert, U.; Huber, L.A. Analysis of CD44-containing lipid rafts: Recruitment of annexin II and stabilization by the actin cytoskeleton. *J Cell Biol* **1999**, *146*, 843-854, doi:10.1083/jcb.146.4.843.
70. Orian-Rousseau, V.; Ponta, H. Perspectives of CD44 targeting therapies. *Arch Toxicol* **2015**, *89*, 3-14, doi:10.1007/s00204-014-1424-2.
71. Menke-van der Houven van Oordt, C.W.; Gomez-Roca, C.; van Herpen, C.; Coveler, A.L.; Mahalingam, D.; Verheul, H.M.; van der Graaf, W.T.; Christen, R.; Rüttinger, D.; Weigand, S.; et al. First-in-human phase I clinical trial of RG7356, an anti-CD44 humanized antibody, in patients with advanced, CD44-expressing solid tumors. *Oncotarget* **2016**, *7*, 80046-80058, doi:10.18632/oncotarget.11098.
72. Riechelmann, H.; Sauter, A.; Golze, W.; Hanft, G.; Schroen, C.; Hoermann, K.; Erhardt, T.; Gronau, S. Phase I trial with the CD44v6-targeting immunoconjugate bivatuzumab mertansine in head and neck squamous cell carcinoma. *Oral Oncol* **2008**, *44*, 823-829, doi:10.1016/j.oraloncology.2007.10.009.
73. Tijink, B.M.; Buter, J.; de Bree, R.; Giaccone, G.; Lang, M.S.; Staab, A.; Leemans, C.R.; van Dongen, G.A. A phase I dose escalation study with anti-CD44v6 bivatuzumab mertansine in patients with incurable squamous cell carcinoma of the head and neck or esophagus. *Clin Cancer Res* **2006**, *12*, 6064-6072, doi:10.1158/1078-0432.Ccr-06-0910.
74. Casucci, M.; Nicolis di Robilant, B.; Falcone, L.; Camisa, B.; Norelli, M.; Genovese, P.; Gentner, B.; Gullotta, F.; Ponzoni, M.; Bernardi, M.; et al. CD44v6-targeted T cells mediate potent antitumor effects against acute myeloid leukemia and multiple myeloma. *Blood* **2013**, *122*, 3461-3472, doi:10.1182/blood-2013-04-493361.
75. Porcellini, S.; Asperti, C.; Corna, S.; Cicoria, E.; Valtolina, V.; Stornaiuolo, A.; Valentinis, B.; Bordignon, C.; Traversari, C. CAR T Cells Redirected to CD44v6 Control Tumor Growth in Lung and Ovary Adenocarcinoma Bearing Mice. *Front Immunol* **2020**, *11*, 99, doi:10.3389/fimmu.2020.00099.
76. Kato, Y.; Kaneko, M.K. A cancer-specific monoclonal antibody recognizes the aberrantly glycosylated podoplanin. *Sci Rep* **2014**, *4*, 5924, doi:10.1038/srep05924.
77. Kaneko, M.K.; Nakamura, T.; Kunita, A.; Fukayama, M.; Abe, S.; Nishioka, Y.; Yamada, S.; Yanaka, M.; Saidoh, N.; Yoshida, K.; et al. ChLpMab-23: Cancer-Specific Human-Mouse Chimeric Anti-Podoplanin Antibody Exhibits Antitumor Activity via Antibody-Dependent Cellular Cytotoxicity. *Monoclon Antib Immunodiagn Immunother* **2017**, *36*, 104-112, doi:10.1089/mab.2017.0014.
78. Kaneko, M.K.; Yamada, S.; Nakamura, T.; Abe, S.; Nishioka, Y.; Kunita, A.; Fukayama, M.; Fujii, Y.; Ogasawara, S.; Kato, Y. Antitumor activity of chLpMab-2, a human-mouse chimeric cancer-specific antihuman podoplanin antibody, via antibody-dependent cellular cytotoxicity. *Cancer Med* **2017**, *6*, 768-777, doi:10.1002/cam4.1049.
79. Suzuki, H.; Kaneko, M.K.; Kato, Y. Roles of Podoplanin in Malignant Progression of Tumor. *Cells* **2022**, *11*, 575, doi:10.3390/cells11030575.
80. Kaneko, M.K.; Ohishi, T.; Kawada, M.; Kato, Y. A cancer-specific anti-podocalyxin monoclonal antibody (60-mG(2a)-f) exerts antitumor effects in mouse xenograft models of pancreatic carcinoma. *Biochem Biophys Rep* **2020**, *24*, 100826, doi:10.1016/j.bbrep.2020.100826.
81. Ishikawa, A.; Waseda, M.; Ishii, T.; Kaneko, M.K.; Kato, Y.; Kaneko, S. Improved anti-solid tumor response by humanized anti-podoplanin chimeric antigen receptor transduced human cytotoxic T cells in an animal model. *Genes Cells* **2022**, in press, doi:10.1111/gtc.12972.

82. Chalise, L.; Kato, A.; Ohno, M.; Maeda, S.; Yamamichi, A.; Kuramitsu, S.; Shiina, S.; Takahashi, H.; Ozone, S.; Yamaguchi, J.; et al. Efficacy of cancer-specific anti-podoplanin CAR-T cells and oncolytic herpes virus G47Δ combination therapy against glioblastoma. *Molecular Therapy - Oncolytics* **2022**, *26*, 265-274, doi:https://doi.org/10.1016/j.omto.2022.07.006.

83. Suzuki, H.; Kaneko, M.K.; Kato, Y. Roles of Podoplanin in Malignant Progression of Tumor. *Cells* **2022**, *11*, doi:10.3390/cells11030575.

Supplementary Table S1. The determination of the binding epitope of C44Mab-1 by ELISA.

Peptide	Coding exon*	Sequence	C44Mab-1
CD44p21–40	2	QIDLNITCRFAGVFHVEKNG	–
CD44p31–50	2	AGVFHVEKNGRYSISRTEAA	–
CD44p41–60	2	RYSISRTEAADLCKAFNSTL	–
CD44p51–70	2	DLCKAFNSTLPTMAQMEKAL	–
CD44p61–80	2/3	PTMAQMEKALSIGFETCRYG	–
CD44p71–90	2/3	SIGFETCRYGFIEGHVVIPR	–
CD44p81–100	3	FIEGHVVIPRIHPNSICAAN	–
CD44p91–110	3	IHPNSICAANNTGVYILTSN	–
CD44p101–120	3	NTGVYILTSNTSQYDTYCFN	–
CD44p111–130	3/4	TSQYDTYCFNASAPPEEDCT	–
CD44p121–140	3/4	ASAPPEEDCTSVTDLPNAFD	–
CD44p131–150	4/5	SVTDLPNAFDGPITITIVNR	–
CD44p141–160	4/5	GPITITIVNRDGTRYVQKGE	–
CD44p151–170	5	DGTRYVQKGEYRTNPEDIYP	–
CD44p161–180	5	YRTNPEDIYPSNPTDDDVSS	–
CD44p171–190	5	SNPTDDDVSSGSSSERSSTS	–
CD44p181–200	5	GSSSERSSTSGGYIFYTFST	–
CD44p191–210	5	GGYIFYTFSTVHPIPDEDSP	–
CD44p201–220	5	VHPIPDEDSPWITDSTDRIP	–
CD44p211–230	5/v3	WITDSTDRIPATSTSSNTIS	–
CD44p221–240	5/v3	ATSTSSNTISAGWEPNEENE	–
CD44p231–250	v3	AGWEPNEENEDERDRHLSFS	–
CD44p241–260	v3	DERDRHLSFSGSGIDDDEDF	–
CD44p251–270	v3/v4	GSGIDDDEDFISSTISTTPR	–
CD44p261–280	v3/v4	ISSTISTTPRAFDHTKQNQD	–
CD44p271–290	v4	AFDHTKQNQDWTQWNPSHSN	–
CD44p281–300	v4	WTQWNPSHSNPEVLLQTTTR	–
CD44p291–310	v4/v5	PEVLLQTTTRMTDVDRNGTT	–
CD44p301–320	v4/v5	MTDVDRNGTTAYEGNWNPEA	–
CD44p311–330	v5	AYEGNWNPEAHPPLIHHEHH	–
CD44p321–340	v5	HPPLIHHEHHEEEETPHSTS	–
CD44p331–350	v5/v6	EEEETPHSTSTIQATPSSTT	–

CD44p341–360	v5/v6	TIQATPSSTTEETATQKEQW	–
CD44p351–370	v6	EETATQKEQWFGNRWHEGYR	–
CD44p361–380	v6	FGNRWHEGYRQTPREDSHST	–
CD44p371–390	v6/v7	QTPREDSHSTTGTAAASAHT	–
CD44p381–400	v6/v7	TGTAAASAHTSHPMQGRTTP	–
CD44p391–410	v7	SHPMQGRTTPSPEDSSWTDF	–
CD44p401–420	v7	SPEDSSWTDFFNPISHPMGR	–
CD44p411–430	v7/v8	FNPISHPMGRGHQAGRRMDM	–
CD44p421–440	v7/v8	GHQAGRRMDMDSSHSTTLQP	–
CD44p431–450	v8	DSSHSTTLQPTANPNTGLVE	–
CD44p441–460	v8	TANPNTGLVEDLDRTGPLSM	–
CD44p451–470	v8/v9	DLDRTGPLSMTTQQSNSQSF	–
CD44p461–480	v8/v9	TTQQSNSQSFSTSHEGLEED	–
CD44p471–490	v9	STSHEGLEEDKDHPTTSTLT	+
CD44p481–500	v9/v10	KDHPTTSTLTSSNRNDVTGG	–
CD44p491–510	v9/v10	SSNRNDVTGGRRDPNHSEGS	–
CD44p501–520	v10	RRDPNHSEGSTTLLEGYTSH	–
CD44p511–530	v10	TTLLEGYTSHYPHTKESRTF	–
CD44p521–540	v10	YPHTKESRTFIPVTSAKTGS	–
CD44p531–550	v10	IPVTSAKTGSFGVTAVTVGD	–
CD44p541–560	v10	FGVTAVTVGDSNSNVNRSLS	–
CD44p551–570	v10/16	SNSNVNRSLSGDQDTFHPSG	–
CD44p561–580	v10/16	GDQDTFHPSGGSHTTHGSES	–
CD44p571–590	16	GSHTTHGSESDGHSHGSQEG	–
CD44p581–600	16/17	DGHSHGSQEGGANTTSGPIR	–
CD44p591–606	17	GANTTSGPIRTPQIPEAAAA	–

+, OD655≧0.3; －, OD655<0.1

*The CD44 exon-cording regions are illustrated in Figure 1.

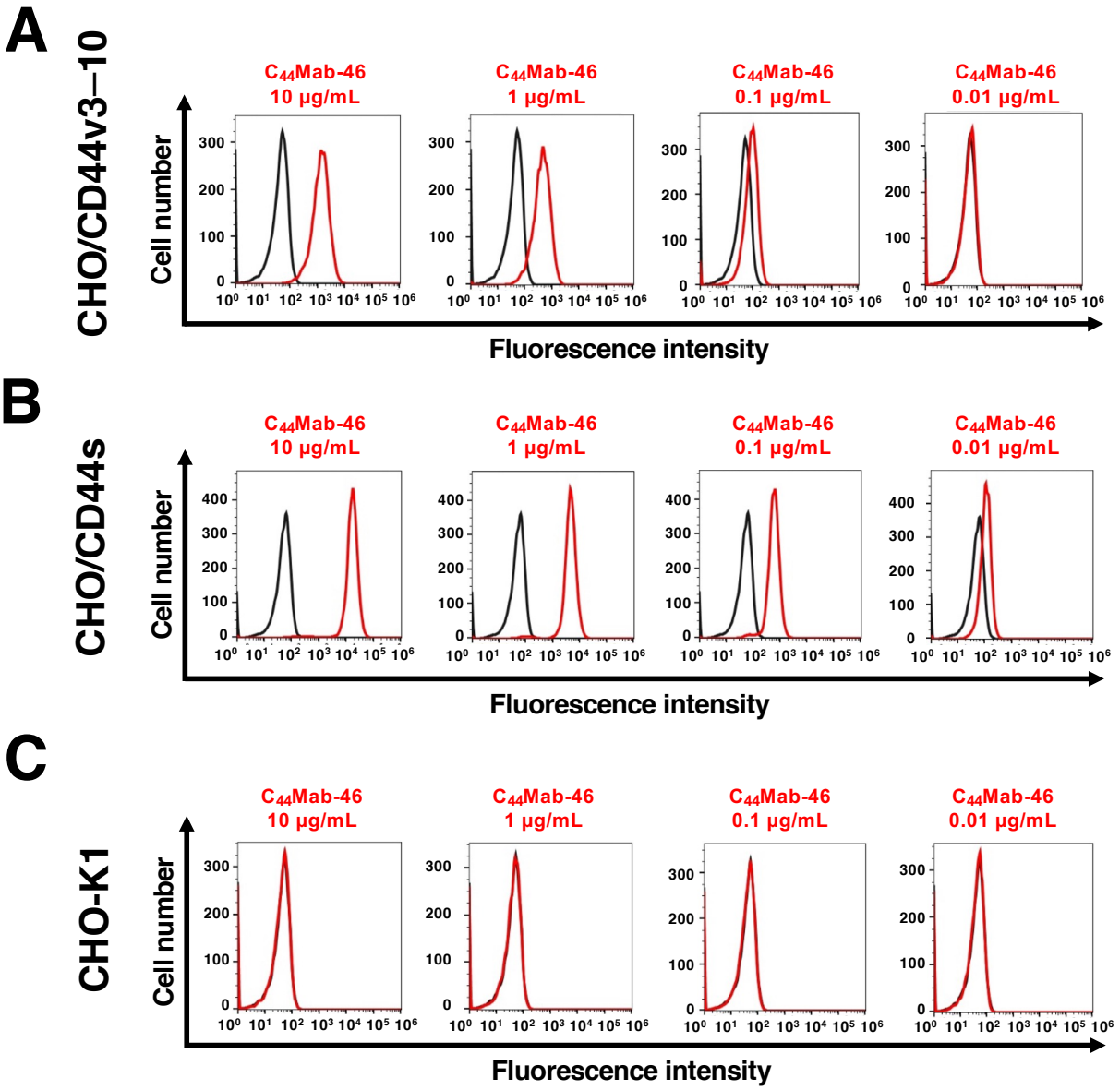

Figure S1 Conformation of the recognition of CHO/CD44s and CHO/CD44v3–10 by C_{44}Mab-46 by flow cytometry. CHO/CD44v3–10 (A), CHO/CD44s (B), and CHO-K1 (C) were treated with 0.01-10 μg/mL of C_{44}Mab-46, followed by treatment with Alexa Fluor 488-conjugated anti-mouse IgG (Red line). The black line represents the negative control (blocking buffer).

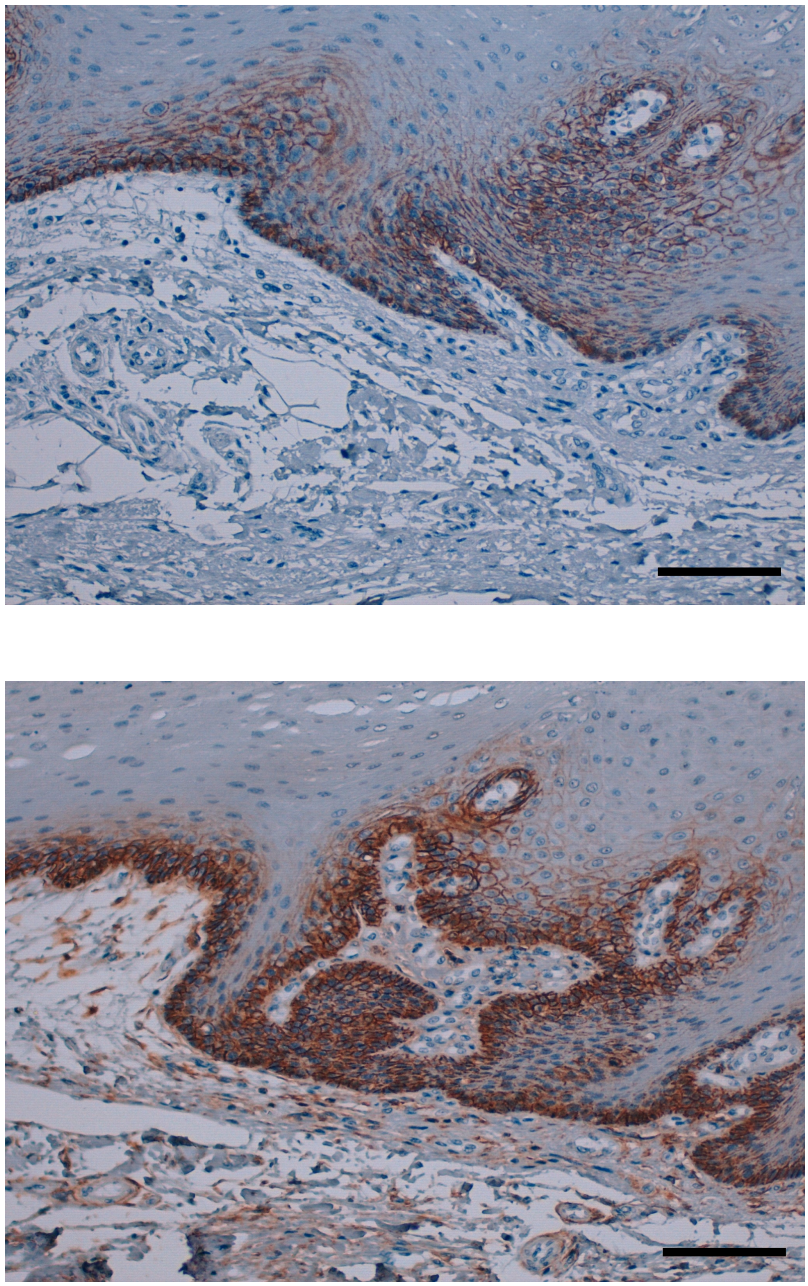

Supplementary Figure S2 Immunohistochemical analysis using C_{44}Mab-1 and C_{44}Mab-46 against oral squamous cell carcinoma tissues. After antigen retrieval, the sections were incubated with 1 μg/mL of C_{44}Mab-1 (A) and 1 μg/mL of C_{44}Mab-46 (B), followed by treatment with the Envision+ kit. The color was developed using 3,3′-diaminobenzidine tetrahydrochloride (DAB), and the sections were counterstained with hematoxylin. Scale bar = 100 μm.